Journal of Engineering Physics and Thermophysics, Vol. 71, No. 1, 1998

EFFECT OF THE TRANSPARENCY OF THE SKELETON ON PARAMETERS OF AN AXISYMMETRIC CYLINDRICAL FILTRATION COMBUSTION HEATER

K. V. Dobrego and S. A. Zhdanok

UDC 536.46

Numerical simulation with a differential approximation of radiation transfer was carried out to study the effect of the partial transparency of the porous skeleton on the radiant efficiency, the maximum temperature, and the localization of the combustion front in an cylindrical axisymmetric filtration combustion heater. It is shown that the partial transparency of amorphous quartz grains for radiation provides a 2–5% increase in the radiant efficiency in comparison with nontransparent materials under the simulated conditions. It is shown that use of transparent fillings can both decrease and increase the skeleton temperature, depending on the size of the system and other parameters. Optical characteristics of porous fillings and models of radiation transfer in isotropic porous media are discussed.

Combustion in a porous body, or filtration combustion (FC) of gases, attracts researchers' interest because of the large number of engineering applications for it. Among them, we can mention recycling (oxidation) of harmful gases, combustion of superlean fuel mixtures in the superadiabatic combustion mode, treatment of catalysts with an adiabatic wave, etc. [1-3]. In recent times, intensive studies have been carried out to investigate heaters that use filtration combustion of gases (FCH). FCH are typically used in thermochemical treatment of metals, ceramics, glass, and semiconductors. A possible configuration of FCH is an axisymmetric cylindrical configuration. With this configuration, fuel is supplied to the center of a ceramic tube and filtered from the center to the external surface. This provides natural stabilization of the combustion front inside the skeleton due to a decrease in the filtration velocity with increase in the radius. The most important problem involved in the study and design of FCH is evaluation of their radiant efficiency and the maximum temperature of the porous skeleton. In view of the fact that porous ceramics differ greatly in their optical properties, determination of the effect of these properties on characteristics of FCH seems of interest.

In what follows we discuss characteristics of porous fillings that serve as the skeleton of an FCH. One-dimensional numerical simulation was conducted to evaluate the effect of the partial transparency of the casing on the radiant efficiency of the FCH, the maximum temperature of the skeleton, and the localization of the combustion front within the skeleton. Radiation transfer is calculated using a differential approximation. The parameters chosen for the calculations are those of a filling of Al_2O_3 (alumina) pellets and amorphous quartz. Results of the study allow optimization of the parameters of the porous material in designing particular devices.

Optical Properties of Porous Bodies. Optical characteristics of porous materials depend on the skeleton material, the surface structure of the solid phase, and the pore size. Some materials such as silicon carbide and asbestos are characterized by a high emissivity factor. Ceramics based on Y_2O_3, MgO, ZrO_2, and some other oxides have rather high transparency for visible and near IR radiation. Y_2O_3 ceramics has the highest transparency in wide visible and IR ranges. Amorphous quartz and special compacted corundum (Al_2O_3) are characterized by a rather high transparency for visible and near IR radiation with a sharp decrease in the transparency at the wavelength $\lambda' \cong 2.7$ μm for quartz and $\lambda' \cong 3$ μm for Al_2O_3. Optical properties of these materials, including the transmission limits, change slightly with increase in the temperature, at least up to $T = 1200^{\circ}C$. Detailed information about thermal and optical properties of ceramics can be found in [4, 5].

Academic Scientific Complex "A. V. Luikov Heat and Mass Transfer Institute of the National Academy of Sciences of Belarus," Minsk, Belarus. Translated from Inzhenerno-Fizcheskii Zhurnal, Vol. 71, No. 1, pp. 62-69, January-February, 1998. Original article submitted June 11, 1997.

1062-0125/98/7101-0059$20.00 ©1998 Plenum Publishing Corporation

TABLE 1. Quantum Mean Free Path l_0 Measured in Terms of the Transmission of the Filling

Filling material	d_0, mm	m	L, mm	Measured l_0, mm
Ground quartz	4	0.42	3.3	4.1
Hollow Al_2O_3 spheres	3	0.38	2.5	3.8
Solid Al_2O_3 spheres	2.8	0.38	2.3	2.3
The same	5.6	0.38	4.7	5.3

In simulation of radiation heat transfer in porous bodies (PB) two approaches are possible in principle, namely, the detailed approach, including the boundary conditions at the phase interface, and the volume-averaged approach, which consists in considering a PB as a continuum with effective optical properties. The former necessitates extraordinarily high computation expenses, while the latter is widely used in simulation of heat transfer in PB, although its theoretical basis requires further investigation. The routine procedure of the volume-averaged simulation includes [6] isolation of a representative element of the porous medium and calculation of cross sections of absorption and scattering at this element with Mie's theory and/or some other methods. In this approach it is assumed that 1) local thermodynamic equilibrium is established, 2) the effect of interference with the surrounding elements is small, and 3) scattering on the element is independent of the structure of its environment (independent scattering) [6-8].

Assumption 2) leads to a limitation from below on the porous-space size L ($L/\lambda' > 0.5$) [7, 8]. It is valid for grains with a diameter of the order of magnitude of millimeters. Although the third assumption imposes limitations on the size of the porous space, it is assumed in [9] that the assumption of independent scattering is not of critical importance for use of the model. Hottel et al. [7] determined that independent scattering occurred at substantial porosity of the PB $m > 0.73$. Kaviany [6] found that the assumption of independent scattering was satisfied well for semitransparent fillings (the optical thickness of a grain $\tau \cong 0.1$), while for nontransparent fillings this assumption was valid for high-porosity systems, but with the porosity $m = 0.4$ it could lead to a severalfold overestimation of the transmissivity of the PB. This behavior can be explained by multiple scattering caused by the presence of surrounding particles. In spite of the fact that conclusions of different authors concerning conditions for satisfaction of assumptions 2) and 3) differ quantitatively, their qualitative content is clear. The problem of local thermodynamic equilibrium of an element of a PB was not discussed in the works mentioned, although at the high temperature gradients in the skeleton that occur at the filtration combustion front, it is violated. Another problem is that in practice it is very difficult to calculate scattering at a representative element even for a monodisperse spherical filling, primarily because of the complicated microporous structure of real ceramics. Therefore, it seems reasonable to use averaged optical characteristics of PB and crude models of optical properties, whenever possible.

A porous body is considered to be a pseudohomogeneous medium that is characterized by the quantum loss coefficient κ and the absorption a and scattering s coefficients, $\kappa = a + s$. Neglecting absorption in the gaseous phase, for nontransparent fillings the quantum mean free path l_0 is assumed to be equal to the mean pore size L and is evaluated from dimensionality considerations as

$$l_0 = L = d_0 \sqrt[3]{m/(1-m)}, \tag{1}$$

although there are other relations in the literature [10, 11] (for highly disperse spongy systems the mean pore size should be evaluated in a different way). Using the familiar emissivity factor of a skeleton material (or the albedo or emissivity, which are related with it), we evaluate the effective absorption and scattering coefficients

$$a = \varepsilon/L, \quad s = (1-\varepsilon)/L, \tag{2}$$

where ε is the integral emissivity factor of the surface of the skeleton material.

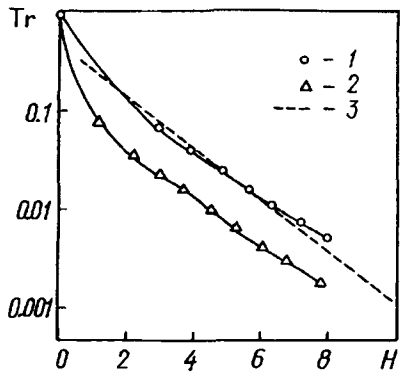

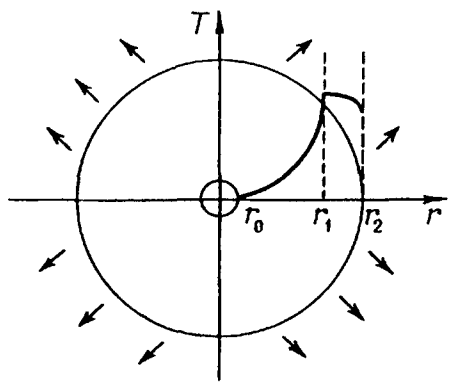

Fig. 1. Normalized integral transmissivity of a filling of borosilicate spheres of $d_0 = 5$ mm versus length of the filling: 1, 2) experimental data of Chen and Churchill [13], $T_0 = 1366$ K and 922 K, respectively; 3) calculated by a DA at $l_0 = 5L$. Tr, dimensionless; H, cm.

Fig. 2. Scheme of an axisymmetric cylindrical FCH. Arrows) radiation and combustion products; solid line) temperature profile of the skeleton.

For transparent (semitransparent) fillings, the quantum mean free path is longer than the mean pore size, although the scattering of radiation due to diffraction, refraction, and interference of passing rays is rather high. In practice, it is reasonable to calculate scattering with Mie's theory or geometric optics [6, 12], if the following conditions are satisfied: 1) in the individual filling material the quantum mean free path greatly (by three or more times) exceeds the length of the pore space; 2) the surface of grains is smooth and slightly scattering; 3) the shapes and size of the grains are regular. Otherwise, it seems reasonable to evaluate roughly the scattering coefficient s in the filling and then compute

$$a = (1 - m)\, a_s, \quad \kappa = s + (1 - m)\, a_s \tag{3}$$

where a_s is the absorption coefficient in the individual material of the solid phase. Otherwise, for transparent fillings the scattering can be neglected in (3). This can be explained by the fact that backscattering at transparent spheres is an order of magnitude lower than at nontransparent ones [13] and that the scattered component hardly participates in energy transfer at substantial optical thicknesses [12].

To evaluate optical properties, for some fillings the quantum mean free path was measured experimentally (Table 1). To this end, specimens of fillings of irregular quartz grains and hollow and solid spheres of nontransparent Al_2O_3 were prepared. A laboratory 0.62-μm He–Ne laser was the light source. A photometer was used as the detector. The thickness of the bed of the filling was varied from 0.5 to 1 cm for the solid spheres and from 1 to 2.5 cm for the hollow spheres and quartz.

As follows from the data given in Table 1, the quantum mean free path in the filling of quartz and hollow Al_2O_3 spheres is longer than the characteristic dimension of the pores, which can be explained by the transmission of the filling. However, this difference is not large because of the high-intensity scattering at rough Al_2O_3 spheres and irregular quartz grains. Substantial transmission of radiation is characteristic of fillings of spherical grains with a smooth (polished) surface. For example, when Chen and Churchill's data [13] obtained for a filling of borosilicate glass spheres 5 mm in diameter are approximated using a differential-approximation (DA) model, the effective quantum mean free path turns out to be 5 times longer than the pore size calculated by means of (1) (Fig. 1). One can also see from the data shown in Fig. 1 that the dependence of the quantum mean free path on the radiation wavelength has a strong effect on the integral transmission, since thermal-radiation transmission with an intensity maximum in the shorter-wave region $\lambda'_{max} \cong 2.1$ μm ($T_0 = 1355$ K) is approximately 3 times higher than thermal-radiation transmission with $\lambda'_{max} \cong 3.1$ μm ($T_0 = 922$ K).

Thus, depending on the size and material of the particles of the porous skeleton, its optical properties can vary substantially, which may affect the distribution of the temperature fields and the operating parameters of the FCH.

Now, we study the dependence of the radiant efficiency, the maximum temperature of the skeleton, and the localization of the combustion front on the quantum mean free path in the skeleton of an axisymmetric cylindrical FCH.

Formulaion of the Problem and Analysis. Consider a one-dimensional axisymmetric cylindrical system (Fig. 2). The gas is assumed to be optically transparent, and the gas flow, isobaric; internal heat sources are neglected, except for gas-phase chemical heat release, which is modeled by the overall Arrhenius reaction.

The mathematical model of the FCH includes the energy equations for the gas and solid phases and the balance equation of the reacting component. With diffusion and heat conduction neglected in the gas phase in comparision with convective flows, we obtain

$$c\rho \frac{\partial T}{\partial t} = \frac{1}{r} \frac{\partial}{\partial r} \lambda r \frac{\partial T}{\partial r} + \nabla q + \alpha (T_g - T), \tag{4}$$

$$c_g \rho_g \frac{\partial T_g}{\partial t} + c_g u_g \frac{\partial T_g}{\partial r} = -\alpha (T_g - T) + QW(y, T_g), \tag{5}$$

$$\rho_g \frac{\partial y}{\partial t} + \rho_g u_g \frac{\partial y}{\partial r} = -\rho_g W(y, T_g). \tag{6}$$

Here ∇q is the divergence of the radiation flow. The subscript g refers to the gas phase, while parameters of the solid phase are given without subscripts. System of equations (4)-(6) is completed by the equation for the chemical-reaction rate, the equation of state of the gas, and the equations for the radiant-energy density and the divergence of the radiation flow in the DA:

$$W(y, T_g) = yz \exp(-15640/T_g), \tag{7}$$

$$\rho_g T_g = \text{const}, \tag{8}$$

$$\nabla \left(\frac{1}{a+s} \right) \nabla U - 4aU + 16a\sigma T^4 = 0, \tag{9}$$

$$\nabla q = 4a\sigma T^4 - c_0 a U, \tag{10}$$

The boundary conditions for Eqs. (4)-(6) and (9) are of the form

$$\left.\frac{\partial T}{\partial r}\right|_{r_0} = 0, \quad \left.\frac{\partial T}{\partial r}\right|_{r_2} = 0; \quad T_g|_{r_0} = T_0; \quad y|_{r_0} = 1; \quad \left.\frac{\partial U}{\partial r}\right|_{r_0} = 0, \quad |q\|_{r_2} = \frac{c_0}{2} U|_{r_2}.$$

The energy supplied to the FCH is determined by the flow rate and enthalpy of the fuel mixture, $Q^+ = GQ$, and is spent on radiation and heating of the combustion products: $Q^+ = Q_{rad} + (c\rho)_g G \Delta T_{2,g}$. If the radiant efficiency of the FCH is defined as the ratio of the energy emitted from the surface as radiation to the energy supplied to the system, some simple manipulations will result in the expression

$$\eta \equiv \frac{Q_{rad}}{Q^+} \cong 1 - \frac{\Delta T_{2,g}}{dT_{ad}} \tag{11}$$

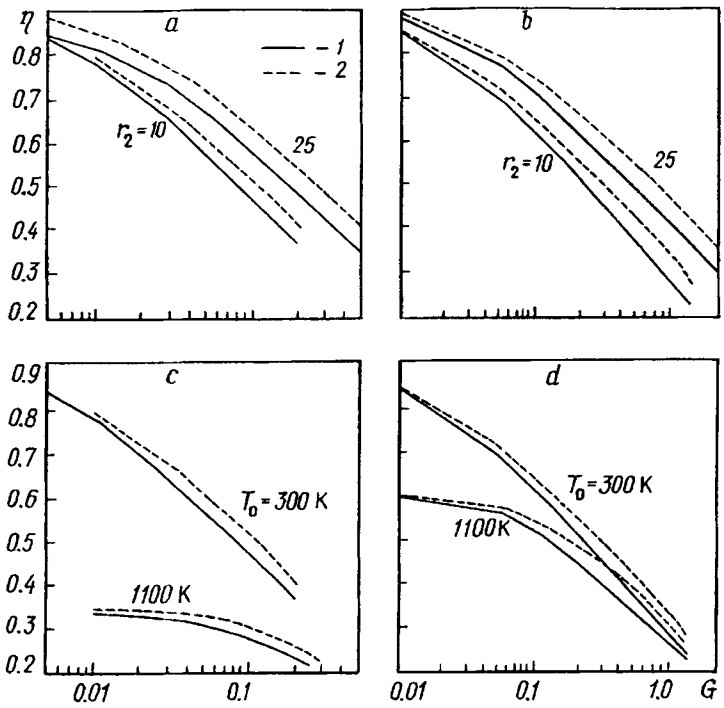

Fig. 3. Plot of the radiant efficiency of FCH made of fillings with different transparencies versus fuel mass flow rate: 1) rough Al_2O_3 spheres, d_0 = 5.6 mm; 2) polished quartz spheres, d_0 = 5.6 mm; a) dT_{ad} = 1200 K, r_2 = 10 and 25 cm, b) dT_{ad} = 2000 K, r_2 = 10 and 25 cm; c) dT_{ad} = 1200 K, r_2 = 10 and 25 cm, T_0 = 300 and 1100 K; d) dT_{ad} = 2000 K, r_2 = 10 cm, T_0 = 300 and 1100 K. η, dimensionless; G, kg/sec·m.

Here $\Delta T_{2,g}$ is the excess of the output-gas temperature over the temperature of the initial gas mixture.

System of equations (4)-(10) together with the boundary conditions was approximated by finite differences and solved in an iteration procedure. Equations (4) and (9) were solved by factorization, while Eqs. (5) and (6) were integrated explicitly. The main series of calculations was carried out for methane–air mixtures with fuel concentrations corresponding to the adiabatic combustion temperatures dT_{ad} = 1200 and 2000 K. The mass flow rate of the mixture per unit length of the FCH was varied in a wide range G = 0.001–2.5 kg/sec·m. Systems with outer radius r_2 = 10 and 25 cm were considered. The thermal conductivity of the skeleton was constant and the other parameters were chosen as follows: λ = 1.5 W/m·K, m = 0.4, and d_0 = 5.6 mm. The interphase heat-transfer coefficient α was taken in accordance with [14]. The calculations were conducted for porous fillings with high (smooth quartz spheres) and low (rough Al_2O_3 grains) radiation transmissivities. The absorption and scattering coefficients were found according to (1) and (2), where ε = 0.6. For the quartz filling the absorption coefficient was taken to be that for a filling of borosilicate glass in [13], and scattering was neglected.

The following characteristics were calculated for both fillings: the radiant efficiency according to formula (11), the maximum temperature of the skeleton, and the steady-state localization of the combustion front (which was determined from the coordinate of the maximal temperature of the gas phase). In the simulation, combustion was initiated inside the FCH, which eliminated uncertainty in localization of the combustion front [15].

In Fig. 3 one can see results of the calculation of the radiant efficiency of the FCH for transparent and nontransparent fillings as a function of the fuel flow rate, fuel caloricity, and dimension (outer radius) of the skeleton of the FCH.

As follows from the calculations, the efficiency of the FCH made of a transparent filling is higher than the efficiency of the nontransparent FCH. This excess $\Delta\eta$ depends slightly on the radius of the FCH and is a little larger for high-calorific fuels (higher dT_{ad}). For the conditions simulated, maximum values of $\Delta\eta$ are given in Table 2. The excess $\Delta\eta$ increases with the fuel rate, has a weakly expressed maximum, and decreases somewhat as the

TABLE 2. Maximum Excess of the Radiant Efficiency $\Delta\eta$ of an FCH Made of a Transparent Quartz Filling over the Radiant Efficiency of an FCH Made of Nontransparent Al_2O_3

r_2, cm	dT_{ad}, K	T_0, K	G, kg/sec·m	$\Delta\eta$, %
10	1200	300	0.1	4.7
25	1200	300	0.1–0.2	5.1
10	1200	1100	0.15–0.2	2.5
25	1200	1100	0.45	2.5
10	2000	300	0.5	5.5
25	2000	300	0.5	5.9
10	2000	1100	0.5	4.8
25	2000	1100	1.5	5

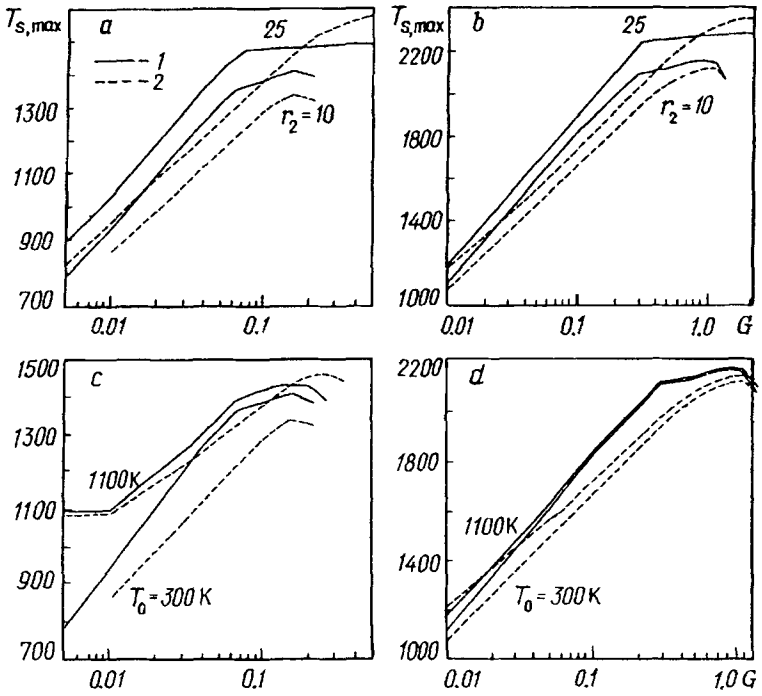

Fig. 4. Plot of the maximum temperature of the skeleton of FCH made of fillings of different transparencies versus fuel mass flow rate: 1, 2, a-d – see Fig. 3.

highest possible fuel rate is approached (Fig. 3a and b). For higher ambient temperatures (typical of heat-treatment furnaces), the maximum is more pronounced on a background of a general decrease in the radiant efficiency.

In Fig. 4 one can see maximum temperatures of the skeleton calculated for transparent and nontransparent filling materials. It follows from the results presented that the maximum temperature $T_{s,max}$ of the transparent skeleton is on average 50–150 K lower than that of the nontransparent skeleton (for the conditions simulated). For higher-calorific fuels this excess is usually somewhat higher than for lean fuel mixtures. However, the graphs show that as the fuel flow rate, the fuel caloricity, and the size of the FCH increase, the maximum temperatures for the transparent and nontransparent fillings approach each other, while for an FCH with a longer radius (r_2 = 25 cm), the situation is the opposite, i.e., $T_{s,max}$ of the transparent skeleton is higher than $T_{s,max}$ of the nontransparent one. This situation can be explained by the fact that for transparent fillings, together with higher radiant heat losses from the combustion front (in comparison with nontransparent ones), more heat is also transfered to the main gas flow, which leads to higher heat recuperation, a higher maximum temperature, and, as

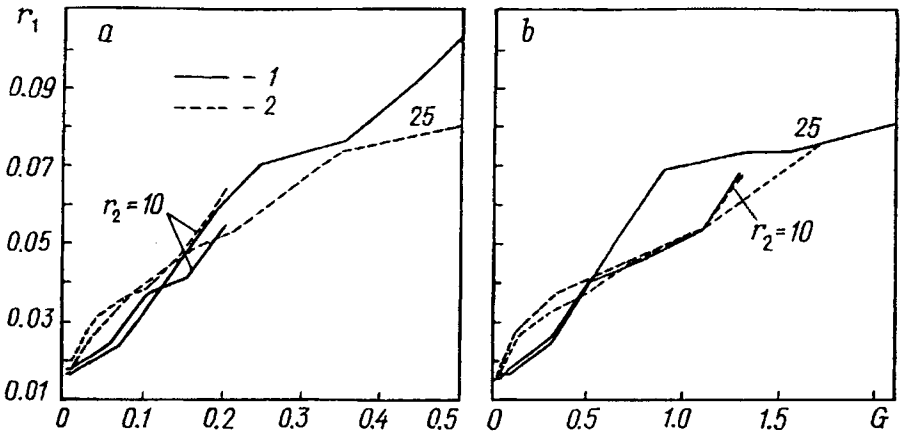

Fig. 5. Plot of the radius of the combustion front in FCH made of fillings with different transparencies versus fuel mass flow rate: 1) rough Al_2O_3 spheres, $d_0 = 5.6$ mm; 2) polished quartz spheres, $d_0 = 5.6$ mm: a) $dT_{ad} = 1200$ K, $T_0 = 300$ K, $r_2 = 10$ and 25 cm; b) $dT_{ad} = 2000$ K, $T_0 = 300$ K, $r_2 = 10$ and 25 cm. r_1, m.

a result of interphase heat transfer, a higher temperature of the skeleton and a countershift of the localization of the combustion front. Since the heat recuperation processes and the heat losses from the front compete and have opposite effects on the temperature of the skeleton, a nontrivial dependence of the maximum temperature of the skeleton on the size of the FCH, the caloricity of the mixture, and other parameters holds, which can be seen in Fig. 4. In particular, for $r_2 = 10$ cm and $T_0 = 300$ K, the maximum temperature of the transparent skeleton is lower than that of the nontransparent skeleton at any fuel flow rates, while at $T_0 = 1100$ K this relation changes at high rates. For an FCH with a longer radius, the maximum temperature of the transparent skeleton exceeds $T_{s,max}$ of the nontransparent skeleton as the fuel mass flow rate increases (Fig. 4a and b).

As follows from Fig. 5, at low fuel flow rates, the combustion front in the transparent skeleton is localized at a longer distance from the center than in the nontransparent skeleton. This can be explained by higher radiation losses from the high-temperature region. As the fuel flow rate increases, depending on the parameters of the system, this situation is either retained, or inverted, which can be related to the appearance of a high-energy radiation flow that is directed opposite to the gas flow and leads to heat recuperation in the system. The inversion of the relation of the maximum temperatures for the transparent and nontransparent skeletons (Fig. 4) corresponds to parameters of the system at which combustion in the transparent skeleton is localized much closer to the center than in the nontransparent skeleton (Fig. 5).

The somewhat nonmonotonic behavior of the combustion localization curves (inflections) shown in Fig. 5 can be related to the effect of a heat sink on the inner and outer radii of the skeleton (boundary conditions) and to the radial changes in the temperature, the gas filtration velocity, and the interphase heat-transfer rate. The problem of localization of the combustion front in similar cylindrical and spherical heaters was considered in [5].

Conclusion. Use of transparent fillings with a quantum mean free path that is several times greater than the pore size results in a 2–5% higher radiant efficiency of the FCH for the parameters of the system that were considered in this article and at ambient room temperature (Fig. 3). At higher ambient temperatures that are typical of metal heat-treatment furnaces, the gain in efficiency obtained from using transparent fillings decreases at low fuel flow rates and for low-calorific fuels. Therefore, use of transparent fillings in FCH intended for heat-treatment furnaces requires feasibility studies that include the thermophysical characteristics discussed in this article.

Transparent fillings result in a 50–150 K decrease in the maximum temperature of the skeleton (heat flux) for the conditions simulated in this work. However, for systems with a larger radius ($r_2 > 10$ cm for the parameters of the system that were considered in this work), because of the higher recuperation efficiency inside the porous skeleton, the temperatures can become closer or the results can even be opposite (Fig. 4). The effect of the increase in heat recuperation obtained in filtration combustion in transparent PB can be used to improve superadiabatic combustion modes.

NOTATION

L, mean pore dimension; d_0, diameter of a grain of the filling of the porous skeleton; m, porosity; l_0, quantum mean free path; κ, a, and s, effective quantum-loss, absorption, and scattering coefficients, respectively; ε, emissivity factor; T, temperature of the skeleton; T_0, ambient temperature; dT_{ad}, temperature increment in adiabatic combustion of the fuel; u_g, average filtration velocity of the gas; Q, thermal effect of the reaction; $W(y, T)$, chemical-reaction rate; y, concentration of the lacking reagent; E, activation energy of the chemical reaction; R, universal gas constant; z, pre-exponent of thr Arrhenius function; c, heat capacity at constant pressure; ρ, bulk density; λ, thermal conductivity; λ', radiation wavelength; λ'_{max}, radiation wavelength at maximum intensity; α, volume heat-transfer coefficient; U, radiant-energy density; q, vector of the radiant energy flux; σ, Stefan–Boltzmann constant; c_0, velocity of light; r, radial coordinate; r_0, r_1, r_2, inner radius of the FCH, radius of the combustion front, and outer radius, respectively; Tr, normalized transmissivity of the bed of filling; H, length of the bed of filling. Subscripts: g, gas phase; s, solid phase; max, maximum value.

REFERENCES

1. F. J. Weinberg, Nature, No. 233, 239-241 (1971).
2. Yu. Sh. Matros, Propagation of Thermal Waves in Heterogeneous Media [in Russian], Novosibirsk (1988).
3. J. R. Howell, M. J. Hall, and J. L. Ellzey, Progress in Energy and Combustion Science, 22, 122-145 (1996).
4. V. P. Balkevich, Technical Ceramics [in Russian], Moscow (1984).
5. R. E. Krzhizhanovskii and Z. Yu. Shtern, Thermal Properties of Nonmetal Materials (Oxides). Reference Book [in Russian], Leningrad (1973).
6. M. Kaviany, Principles of Heat Transfer in Porous Media, New York (1991).
7. H. C. Hottel, A. F. Sarofim, W. H. Dalzell, and I. A. Vasalos, AIAA J., 9, 1895-1899 (1971).
8. Y. Yamada, J. D. Cartigny, and C.- L. Tien, ASME J. Heat Transfer, 108, 614-620 (1986).
9. M. Q. Brewster and C.-L. Tien, ASME J. Heat Transfer, 104, 573-579 (1982).
10. N. V. Pavlyukevich, Inzh.-Fiz. Zh., 59, No. 4, 606-609 (1990).
11. J. D. Verschoor and P. Greeber, Trans. ASME, 74, 961-968 (1952).
12. R. Siegel and J. Howell, Radiation Heat Transfer [Russian translation], Moscow (1975).
13. J. C. Chen and S. W. Churchill, AIChE J., 9, No. 1, 35-41 (1963).
14. M. E. Aerov, O. M. Todes, and D. A. Narinskii, Apparatus with a Stationary Granular Bed [in Russian], Moscow (1979).
15. K. V. Dobrego, S. A. Zhdanok, and S. I. Futko, Int. J. Heat Mass Transfer, 41 (1998).